

Prediction and analysis of optimal frequency of layered composite structure using higher-order FEM and soft computing techniques

Arijit Das^{1a}, Chetan K. Hirwani^{1b}, Subrata K. Panda^{*1}, Umut Topal^{2c} and Tayfun Dede^{3d}

¹Department of Mechanical Engineering, National Institute of Technology Rourkela, Rourkela: 769008, India

²Department of Civil Engineering, Faculty of Technology, Karadeniz Technical University, Trabzon, Turkey

³Department of Civil Engineering, Karadeniz Technical University, Trabzon, Turkey

(Received August 2, 2018, Revised November 23, 2018, Accepted December 2, 2018)

Abstract. This article derived a hybrid coupling technique using the higher-order displacement polynomial and three soft computing techniques (teaching learning-based optimization, particle swarm optimization, and artificial bee colony) to predict the optimal stacking sequence of the layered structure and the corresponding frequency values. The higher-order displacement kinematics is adopted for the mathematical model derivation considering the necessary stress and strain continuity and the elimination of shear correction factor. A nine-noded isoparametric Lagrangian element (eighty-one degrees of freedom at each node) is engaged for the discretisation and the desired model equation derived via the classical Hamilton's principle. Subsequently, three soft computing techniques are employed to predict the maximum natural frequency values corresponding to their optimum layer sequences via a suitable home-made computer code. The finite element convergence rate including the optimal solution stability is established through the iterative solutions. Further, the predicted optimal stacking sequence including the accuracy of the frequency values are verified with adequate comparison studies. Lastly, the derived hybrid models are explored further to by solving different numerical examples for the combined structural parameters (length to width ratio, length to thickness ratio and orthotropy on frequency and layer-sequence) and the implicit behavior discussed in details.

Keywords: laminated composite; TLBO; PSO; ABC; HSDT; optimization

1. Introduction

The increased demand for the advanced composite materials in several industries (aircraft, submarine, automobiles, building construction, communication and safety equipment) requires a comprehensive understanding of the structural component before the final finished product. The recent study shows that the composite market has been increased steeply worldwide and in particular the developed nation (the utilization raised by 6.3% in 2014 to reach \$8.2 billion market price Mallick, 2007 at the United States). Owing to the structural flexibility and corresponding strength to weight ratios are the primary demands for most weight sensitive applications. Advanced composites have largely occupied the market since their inception in 1950's when merely 2-3% (Boeing 707's structure) components made of composite (Stewart 2009) whereas the current application jumps 50%. Hence, to satisfy the increased demand of the future as well as the current market, it is essential to predict the performance of

composite components, before the large-scale fabrication. The composite structural components are generally associated with the inherent risks and the uncertainty, hence, the accurate modeling may lead to the economic and hassle-free process. For this, it is prudent to carry out the computer-aided analysis in conjunction with the well-known soft computing technique may help in unpleasant losses. Additionally, these structural components generally exposed to the dynamic type of load during the operational life and therefore leads to the vibrational fatigue. Hence, it is necessary to design the components not only for the strength purpose but also capable of withstanding the vibrational fatigue. The soft computing techniques are generally adopted for the optimization of the complex structural responses including the associated parameter (geometry, stacking sequence and environment for composite) where traditional methods unable to achieve the desired values.

The optimal structural parameter has been computed via different soft computing techniques in the past to describe the best possible design input values for the final layered structure. Rao *et al.* (2011) developed first-time a teaching learning-based optimization (TLBO) technique heuristically to make a progress step-wise fashion by learning partly from the earlier work. This method has been applied successfully to solve different engineering problems such as die casting (Rao *et al.* 2014), fatigue analysis of leaf spring (Sayare and Kamble 2015), machining of carbon fiber reinforced epoxy (Kumar *et al.* 2017) and erosion wear rate

*Corresponding author, Associate Professor,
E-mail: call2subrat@gmail.com; pandask@nitrrkl.ac.in

^aLead Author, Research Scholar,
E-mail: aridas122@gmail.com

^bResearch Scholar, E-mail: chetanhirwani111@gmail.com

^cProfessor, E-mail: utopal@ktu.edu.tr

^dAssociate Professor, E-mail: dtayfun@ktu.edu.tr

optimization of short glass fibers and LD slag filled polypropylene composite (Pati *et al.* 2017) and so on. Similarly, the particle swarm optimization (PSO) technique a metaheuristic method and propelled by the social conducts of bird rushing or fish schooling. The fitness values for all particles are assessed by the objective function to be optimized and have speeds which coordinate the flying of the particles (Eberhart and Shi 2001). The effectiveness of this method has been studied by solving the entropy minimization problem of the heat exchangers (Rao and Patel 2010). Additionally, PSO technique implemented successfully for the optimal frequency evaluation of the laminated composite structure by taking the mid-plane kinematic models either the classical laminate theory (CLPT) (Bargh and Sadr 2012) or the higher-order shear deformation theory (HSDT) (Vosoughi *et al.* 2016). Likewise, the PSO is employed further to examine the structural damage identification (Perera *et al.* 2010) including the truss related cases (Tsavdaridis *et al.* 2015 and Kaveh and Talatahari 2009).

The Artificial Bee Colony (ABC) algorithm is another technique where every food source relates to an answer for the optimization process and the measure of nectar at a food source refers to the fitness of solution. The employed honeybees find their food sources by leading a search in their neighborhood. Onlooker honey bees are enrolled to the food sources in light of their quality values. Top notch solutions have a higher probability for being chosen. The superiority of this method is proven (Karaboga and Basturk 2008) by comparing the result of this method, i.e., ABC with the differential evolution, evolutionary algorithm and PSO methods. The ABC (Apalak *et al.* 2014) and the modified version of ABC (Omkar *et al.* 2011) for discrete variables is also developed and coupled with CLPT to optimize the design variables of the layered composite. In continuation to that, the improved form of the ABC is also utilized for the analysis of the cracked beam structural problem (Ding *et al.* 2017). Further, many research articles related to the weight minimization (Grzywinski 2015 and Vo-Duy *et al.* 2017), frequency maximization (Narita 2006, Apalak *et al.* 2008 and Zhang *et al.* 2014), topology optimisation implementation and stiffness anisotropic effect on additively manufactured component (Chiu *et al.* 2018), thickness optimization (Conti *et al.* 1997) and buckling load optimization (Ho-Huu *et al.* 2016) of the layered and

functionally graded carbon nanotube structures (Vo-Duy 2018) are solved using different available techniques coupled with the CLPT and/or the HSDT (Aagaah *et al.* 2006) type of displacement polynomials. Additionally, 3D elasticity theory is adopted to compute the nano structural responses and the particle influence using the modified theoretical models (Fourn *et al.* 2018, Karami *et al.* 2018 and Menasria *et al.* 2017, Hajmohammad *et al.* 2018, Kolahchi *et al.* 2017a, b, Kolahchi 2017, Kolahchi and Cheraghbak 2017, Kolahchi and Bidgoli 2016) including the prediction of optimal buckling load (Kolahchi *et al.* 2017a, b).

The review of the articles indicates that the different optimization techniques have already been developed in the past including the mid-plane theories for the analysis and the prediction of the preferred parameter to design final finished structural components made of composite material (beam and plate). Also, we note that a comprehensive amount of literature discussed on either the CLPT or the FSDT kinematic models including the optimal technique instead of the HSDT type of displacement polynomial model (approximation for the d). Hence, the authors of the present research attempted first-time to derive a new coupled (higher-order kinematic model including different optimization algorithms, i.e., TLBO, PSO and ABC technique) FE model for the prediction of frequency responses by optimizing the fiber orientations assuming the frequency maximization. The numerical model stability established as a priori and extended to evaluate the defined responses for variable input parameter including the influence of selected optimal technique. Subsequently, the inferences of each parameter on the optimal structural frequencies are computed via different numerical examples and presented in details.

2. Theoretical formulation

The plate model has been established with the assumption that the plate is composed of the finite number of orthotropic layers of uniform thickness as depicted in Fig. 1. The dimensions of the plate are, i.e., length l_1 , width l_2 in x_1 and x_2 direction, respectively and thickness is l_3 in x_3 direction.

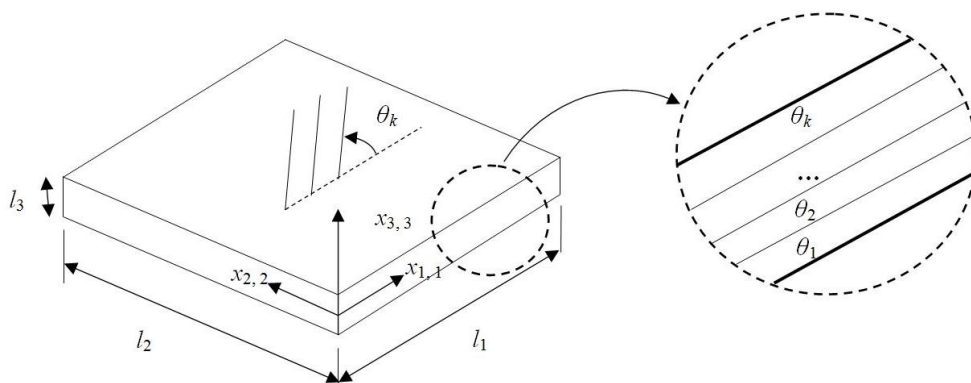


Fig. 1 Representation of the laminated composite plate

2.1 Displacement field

In this study, a higher-order shear deformation model has been utilized for the modeling of a laminated composite plate. The displacement field is considered as same as in the source (Patle *et al.* 2018) (the displacement variation throughout the thickness is assumed to be constant thus giving zero transverse normal strain)

$$\left. \begin{aligned} \bar{u}(x_1, x_2, x_3) &= u(x_1, x_2) + x_3 \theta_1(x_1, x_2) + x_3^2 \lambda_1(x_1, x_2) + x_3^3 \psi_1(x_1, x_2) \\ \bar{v}(x_1, x_2, x_3) &= v(x_1, x_2) + x_3 \theta_2(x_1, x_2) + x_3^2 \lambda_2(x_1, x_2) + x_3^3 \psi_2(x_1, x_2) \\ \bar{w}(x_1, x_2, x_3) &= w(x_1, x_2) \end{aligned} \right\} \quad (1)$$

Here, the displacement of any arbitrary point in the plate geometry is defined as \bar{u} , \bar{v} and \bar{w} along x_1 , x_2 and x_3 direction. Additionally, the above-mentioned equation associated with u , v and w are the mid-plane displacement values and the rotations i.e., θ_1 and θ_2 are the rotation of normal to the mid-plane about x_2 and x_1 direction, respectively. The remaining terms θ_3 , λ_1 , λ_2 , ψ_1 and ψ_2 are the higher-order terms included from Taylor's series expansion to maintain the desired parabolic distribution of shear stress through the entire thickness of the plate.

2.2 Constitutive relation

For any k^{th} layer laminae, the stress-strain relationship (Jones 1999) is expressed mathematically as below by considering an arbitrary angle ' θ ' of the fiber orientation as

$$\{\sigma_{ij}\} = [\bar{Q}_{ij}] \{\varepsilon_{ij}\} \quad (2)$$

where, $\{\sigma_{ij}\}$, $[\bar{Q}_{ij}]$ and $\{\varepsilon_{ij}\}$ are the stress matrix, the elastic property matrix and the strain matrix respectively. Further, the elastic property matrix and strain matrix can be explored as

$$[\bar{Q}_{ij}] = \begin{bmatrix} \bar{Q}_{11} & \bar{Q}_{12} & 0 & 0 & \bar{Q}_{16} \\ \bar{Q}_{12} & \bar{Q}_{22} & 0 & 0 & \bar{Q}_{26} \\ 0 & 0 & \bar{Q}_{44} & \bar{Q}_{45} & 0 \\ 0 & 0 & \bar{Q}_{54} & \bar{Q}_{55} & 0 \\ \bar{Q}_{16} & \bar{Q}_{26} & 0 & 0 & \bar{Q}_{66} \end{bmatrix} \quad (3)$$

$$\{\varepsilon_{ij}\} = \begin{bmatrix} \varepsilon_{x_1 x_1} \\ \varepsilon_{x_2 x_2} \\ \gamma_{x_2 x_3} \\ \gamma_{x_1 x_3} \\ \gamma_{x_1 x_2} \end{bmatrix} = \begin{pmatrix} \frac{\partial \bar{u}}{\partial x_1} & \frac{\partial \bar{v}}{\partial x_2} & \frac{\partial \bar{v}}{\partial x_3} + \frac{\partial \bar{w}}{\partial x_2} & \frac{\partial \bar{u}}{\partial x_3} + \frac{\partial \bar{w}}{\partial x_1} & \frac{\partial \bar{u}}{\partial x_2} + \frac{\partial \bar{v}}{\partial x_1} \end{pmatrix} \quad (4)$$

2.3 Finite element formulation

FEM provides accurate numerical solutions for critical engineering problems with least possible errors. Hence, in the current analysis the geometry is modeled with FEM using an isoparametric quadrilateral Lagrangian element and nine degrees of freedom per node for the accurate prediction of the final solution. The displacement vector at

any point on the mid-surface for the discussed model is given by

$$\{\delta\} = [u \ v \ w \ \theta_1 \ \theta_2 \ \lambda_1 \ \lambda_2 \ \psi_1 \ \psi_2]^T = \sum_{i=1}^9 [N_i] \{\delta_i\} \quad (5)$$

$[N_i]$ represents the interpolation function and the displacement field vector for the i^{th} node as $\{\delta_i\}$. The nodal points generally signify the physical characteristics and the shape functions of the current element (Cook *et al.* 2003). Now, the mid-plane strain vector can be written as

$$\{\varepsilon\}_i = [B_i] \{\delta_i\} \quad (6)$$

where, $[B_i]$ represents the strain displacement relation matrix in accordance with the type of model.

2.4 Energy of the panel

The strain energy (S) of the laminate can be expressed as

$$S = \frac{1}{2} \iint \left[\int_{-h/2}^{+h/2} \{\varepsilon\}^T \{\sigma\} dx_3 \right] dx_1 dx_2 \quad (7)$$

Similarly, the kinetic energy (V) of the free vibrated composite panel can be expressed as

$$V = \frac{1}{2} \iint \left\{ \sum_{k=1}^N \int_{x_{3k-1}}^{x_{3k}} \rho^k \left\{ \dot{d} \right\}^T \left\{ \dot{d} \right\} dx_3 \right\} dx_1 dx_2 \quad (8)$$

where, expression ρ and $\{\dot{d}\}$ denotes the mass density and the velocity vector, respectively.

The elemental stiffness matrix ($[K]$) and the mass matrix ($[M]$) can be expressed as following

$$\begin{aligned} [K] &= \int_A \left(\sum_{k=1}^n \int_{x_{k-1}}^{x_k} [B_L]^T [D] [B_L] dx_3 \right) dA \\ [M] &= \int_A \left(\sum_{k=1}^n \int_{x_{k-1}}^{x_k} [N]^T [N] \rho dx_3 \right) dA \end{aligned} \quad (9)$$

2.5 Governing equations and solution technique

Now, the governing equation is obtained by reducing the order of the total energy using to Hamilton's principle and denoted as in (Cook *et al.* 2003)

$$\delta \int_{t_1}^{t_2} (V - S) dt = 0 \quad (10)$$

Substituting Eqs. (7) and (8) into Eq. (9), the final form of the equation will be conceded as

$$[M] \left\{ \ddot{\delta} \right\} + [K] \{\delta\} = 0 \quad (11)$$

where, $\ddot{\delta}$ is the acceleration, δ is the displacement.

The natural frequency of the system is computed from

Table 1 Plate edge constraints

Conditions	at $x_1=0, l_1$	at $x_2=0, l_2$
Simply-support (S):	$\left. \begin{array}{l} v \\ w \\ \theta_2 \\ \lambda_2 \\ \psi_2 \end{array} \right\} = 0$	$\left. \begin{array}{l} u \\ w \\ \theta_1 \\ \lambda_1 \\ \psi_1 \end{array} \right\} = 0$
Clamped (C):	$u = v = w = \theta_1 = \theta_2 = \lambda_1 = \lambda_2 = \psi_1 = \psi_2 = 0$	
Free (F):	$u \neq v \neq w \neq \theta_1 \neq \theta_2 \neq \lambda_1 \neq \lambda_2 \neq \psi_1 \neq \psi_2 \neq 0$	

the eigenvalue solution of the proposed equation and summarised as

$$([K] - \omega^2 [M])\Delta = 0 \quad (12)$$

where ω and Δ are the natural frequency and the corresponding eigen vector, respectively.

Eq. (12) is solved by using the given sets of boundary conditions shown in Table 1 to avoid rigid body movements and to reduce the number of unknowns.

2.6 Algorithms

2.6.1 Teaching learning based optimization

Teaching-learning is an important process where the objective is achieved through the learning from each step to improve the initial knowledge. Rao *et al.* (2011) proposed an algorithm, known as Teaching-Learning-Based Optimization (TLBO), which simulates the traditional teaching-learning phenomenon of a classroom. The algorithm simulates two fundamental modes of learning: (i) teaching phase; and (ii) learning phase. TLBO is a population based algorithm, where a group of students (i.e., learner) is considered the population and the different subjects offered to the learners are analogous with the different design variables of the optimization problem. The results of the learner are analogous to the fitness value of the optimization problem. The best solution in the entire population is considered as the teacher.

2.6.2 Teaching phase

Teacher phase is the initial phase which involves a tutor who imparts his knowledge to the learners to increase the average marks M_1 of his students to a higher value M_2 . It is assumed that at any particular iteration k there are ' m ' number of subjects which are being taught to ' l ' number of learners and M_j is the average result of the students in any subject. The latest average marks M_{new} considering all subjects is assumed to be the result of the best student ψ_{best} . Now, the difference between the current average result and M_{new} can be computed via following formulae

$$Diff_Mean_k = \phi_i (M_{new} - T_f M_s) \quad (13)$$

Here, M_{new} is the best average obtained, ϕ_i is any

random number and T_f is the teaching factor ranging from 0 to 1.

$$T_f = \text{round} [1 + \text{rand}(0,1) \{2-1\}] \quad (14)$$

Further, the existing solution is modified by adding the aforesaid difference as

$$\chi_{new,j} = \chi_{old,j} + Diff_Mean_j \quad (15)$$

2.6.3 Learning phase

This phase of the algorithm simulates the learning of the students (i.e., learners) through interaction among themselves. The students can also gain knowledge by discussing and interacting with other students. A learner will learn new information if the other learners have more knowledge than him or her. The learning phenomenon of this phase is expressed below:

```

for i = 1: Mnew
    Select any student randomly (Xj, i ≠ j)
    if Xi is better than Xj
        Xnew = Xold + rand*(Xi - Xj)
    else
        Xnew = Xold + rand*(Xj - Xi)
    end
    if Xnew is better than Xold
        Xi = Xnew
    end if
end for

```

The step-wise procedure for the implementation of TLBO is given as below:

Step 1 generate initial population randomly

Step 2 calculate the mean of each design variable, i.e. $mean(X_i) = (\sum_{j=1}^{M_{new}} X_{i,j}) / M_{new}$

Step 3 define a student as a teacher whose objective function (f) is maximum

Step 4 update all student by using Eq. (13)

Step 5 compared students with each other (see computer code given in the section 3.1.2)

Step 6 is the termination criteria satisfied, if no, go to step 2.

Step 7 find the student whose objective function (f) is maximum and assign it as best solution

The total number of function evaluation of the TLBO is calculated as $2 * G_n * P_n + P_n$, where “ G_n ” is the number of the iteration. However, the TLBO is an efficient algorithm to find global optimal solutions of the optimization problem. The later phase of the algorithm is dedicated for increasing the knowledge of students by group interactions. A student interacts randomly with his other fellow mates to upgrade his or her knowledge. Considering two separate learners χ_i and χ_j where $i \neq j$ at any iteration k

$$\begin{aligned} \chi_{new,k} &= \chi_{old,k} + \phi_i(\chi_i - \chi_j) & \text{if } f(\chi_i) < f(\chi_j) \\ \chi_{new,k} &= \chi_{old,k} + \phi_i(\chi_j - \chi_i) & \text{if } f(\chi_j) < f(\chi_i) \end{aligned} \quad (16)$$

χ_{new} gets accepted whenever a better feasible solution is obtained.

2.6.4 Artificial bee colony optimization

In this optimization technique, the behavior of honey bees is manifested for predicting optimal solutions. There are two groups of the bees viz. employed bees and onlookers who take part in the process. The number of food sources around hive is assumed to be the number of employed bees. When the food source gets exhausted, an employed bee becomes a scout bee. The algorithm is subdivided into four phases; the first one is the initialization phase:

The expression for random generation of the food source is shown below

$$\lambda_{m,j} = \beta_j + rand(0,1) \times (\alpha_j - \beta_j) \quad (17)$$

Where, m is the dimension, α_j and β_j are higher and lower extreme boundaries of a solution of the objective function, $rand(0, 1)$ gives any random number within limits $[0, 1]$. The second phase is the employed bees' phase in which the neighbor food source $\tau_{m,j}$ is determined and calculated by the following equation.

$$\tau_{m,j} = \lambda_{m,j} + \phi_{m,j} \times (\lambda_{m,j} - \lambda_{k,j}) \quad (18)$$

where, j is an arbitrary parameter index, λ_j is an arbitrary selected food source, $\phi_{m,j}$ is a random number within the limits $[-1, 1]$. The objective function value (fitness) is evaluated as follows and a selection is made between λ_m and τ_m

$$fit(\lambda_m) = \begin{cases} \frac{1}{1 + f(\lambda_m)}, & f(\lambda_m) \geq 0 \\ 1 + |f(\lambda_m)|, & f(\lambda_m) \leq 0 \end{cases} \quad (19)$$

The third phase is that of the onlooker bees' phase where the amount of food source is judged by its profitability and the profitability of all food sources δ_m is determined by the formula

$$\delta_m = \frac{fit_m(\lambda_m)}{\sum_{m=1}^{SN} fit_m(\lambda_m)} \quad (20)$$

where, $fit(\lambda_m)$ is the fitness of onlooker bees in the neighborhood of food source according to the expression

$$\lambda_m = \beta_i + rand(0,1) \times (\alpha_i - \beta_i) \quad (21)$$

Scout bees' or the final phase: If the food source couldn't change after the limit mentioned above, the food source will be abandoned and Eq. (17) is used to replace that food source.

2.6.5 Particle swarm optimization

This technique is developed on the basis of swarm intelligence heuristics which simulate the food searching patterns and corresponding behavior of few selective creatures in nature. Out of the available techniques, PSO imitates the behavior of a congregation of birds or fishes. In this method, a population is iteratively modified until a termination criteria puts an end to it. In PSO, the entire population $K = \{K_1, K_2, \dots, K_n\}$ of feasible answers is referred to as a swarm where K_1, K_2, \dots, K_n represented as particles. This method does not modify the population in successive iterations but tries to maintain the initial population and update the positions of those particles after each iteration. There is no such concept of the survival of the fittest and particles do not mutate or regenerate as prominent in the genetic algorithms, but the particles interact among themselves and the better solutions are replaced with the inferior ones.

In general, four variables associated with any particle presented in the form of subscript ' j ' at any particular iteration and superscript ' k ' are showing: $\zeta_j^{(k)}$, $\lambda_j^{(k)}$, $\gamma_j^{(k)}$ and $v_j^{(k)}$ are the current position vector, the previous best position, the previous best position of the surrounding particles and the particle speed, respectively. Initially, the particle positions are randomly organized, and the velocities are set as null or small random values. In this algorithm, the user has to input certain parameters like $\varepsilon^{(k)}$ which is the inertia weight or a damping factor whose value decreases approximately from 0.9 to 0.4 during iterations. ϕ_1 , ϕ_2 are acceleration coefficients whose values lie approximately between 0 to 4. The model for particle update speed in the current analysis is mentioned below

$$v_k^{(k+1)} = \varepsilon^{(k)} v_i^{(k)} + \phi_1 \eta_1 (\lambda_j^{(k)} - \zeta_j^{(k)}) + \phi_2 \eta_2 (\gamma_j^{(k)} - \zeta_j^{(k)}) \quad (22)$$

where, η_1 and η_2 denote random numbers of uniform distribution. The three sections of the velocity of Eq. (22) are the inertia, cognitive behavior of present particle and surrounding particles, respectively. Position at any iteration k changes according to the following equation

$$\zeta_j^{(k+1)} = \zeta_j^{(k)} + v_j^{(k+1)} \quad (23)$$

3. Results and discussion

The mathematical formulation discussed in the above section is now converted into a MATLAB code to obtain the necessary dynamic responses and corresponding layer

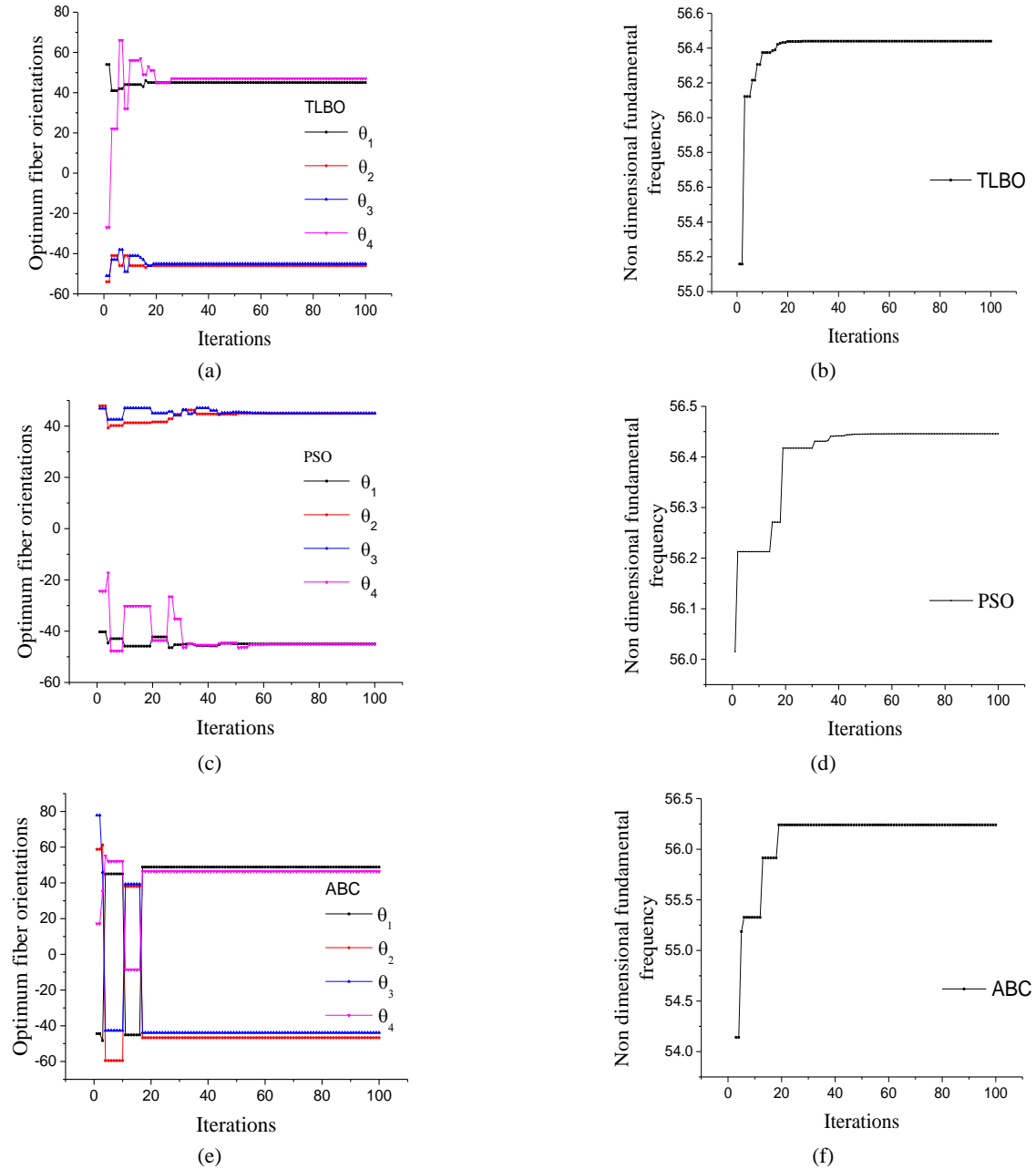


Fig. 2 Convergence study of the simply-supported eight-layer antisymmetric angle-ply square plate ($l_1/l_3 = 20$, $E_1/E_2 = 25$).

sequences. The non-dimensional form of the fundamental frequency and the material property as presented below throughout the study else stated otherwise.

Nondimensional frequency:

$$\Omega = \omega l_1^2 \left(\frac{\rho_0}{D_o} \right)^{1/2}$$

where the reference bending rigidity D_o is given by:
 $D_o = E_2 l_3^3 / 12(1 - \nu_{12}\nu_{21})$.

Material Properties (Bargh and Sadr 2012)

$$E_1 = 138 \text{ GPa}, E_2 = 8.96 \text{ GPa}, G_{12} = G_{13} = 7.1 \text{ GPa}, \\ G_{23} = 3.55 \text{ GPa}, \nu_{12} = \nu_{13} = \nu_{23} = 0.3.$$

The problem involves finding the best orientation of

fiber angles which maximizes the non-dimensional frequency, Ω . The symmetric condition is enforced by optimizing only one half of the laminated structure. The optimal design problem is stated as:

Find: $\theta = (\theta_1, \theta_2, \dots, \theta_k)$
 To maximize: $\Omega = \Omega(\theta_1, \theta_2, \dots, \theta_k)$
 θ_k is subjected to $-90^\circ \leq \theta_k \leq 90^\circ$
 k is half of the layer number

3.1 Performance check of the hybrid model

The necessary performance check (convergence and comparison) of the currently developed computer code is performed in this section. For the convergence study, a square ($l_1/l_2 = 1$) simply-supported eight-layered laminated

composite plate ($l_1/l_3 = 20$) is considered. The material property is taken as defined above except, $E_1 = 25 E_2$. The necessary responses, i.e., nondimensional frequency and laminae orientations are obtained using all three kind of models (TLBO, PSO and ABC) and presented in Fig. 2. It infers from the figure that all the four orientations, as well as the frequency values, are almost stable from the 20th iterations.

Now, for the comparison study, the eight-layered antisymmetric plate structure is analyzed for different edge conditions; CCCF, SSSS, SSSF, SFSF and SSCC. The notations, C, S and F stand for the clamped, the simply-supported, and the free edge of the plate, respectively. For the edge condition CCCF geometrical parameter parameters are taken as ($l_1/l_2 = 2$, $l_1/l_3 = 100$) and for remaining edge conditions geometrical parameters are considered as ($l_1/l_2 = 1$, $l_1/l_3 = 100$). The responses are calculated for the CCCF end constraint using the current PSO and compared with the source values obtained via the genetic algorithm. The present and the reference data (Bargh and Sadr 2012) provided in Fig. 3 for the comparison purpose. In addition, the responses for the remaining edge constraints are evaluated via the current PSO technique and compared with two techniques (layer-wise optimization and PSO solution technique) as provided in the references (Narita 2006,

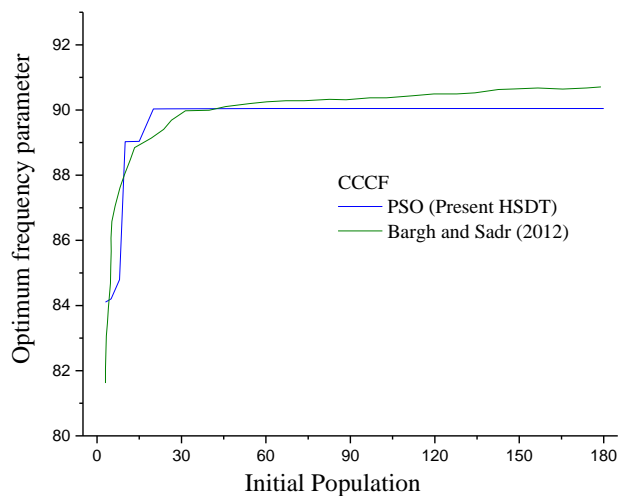


Fig. 3 Comparison of natural frequency of eight-layered rectangular ($l_1 / l_2 = 2$) laminated plate CCCF boundary condition

Bargh and Sadr 2012). The present and the reference values are provided in Table 2. The frequency values including the fibre orientations are obtained using the currently proposed techniques showing good agreement with the reference data.

3.2 New illustrations

After the necessary performance check of the present model, now the model is engaged to compute the frequency parameters for the different parameters to show the model applicability. For the parametric study, an eight-layer square antisymmetric laminated composite plate problem is considered with the defined material properties else stated otherwise. In addition, the geometrical parameters are defined in the description of the respective examples.

3.2.1 Effect of aspect ratio (l_1/l_2)

In this example the nondimensional natural frequency of the simply-supported laminated plate structure ($l_1/l_3 = 100$) is investigated for various length to breadth ratio ($l_1/l_2 = 1$, 1.5, 2, 2.5 and 3). The said responses are obtained using all the three algorithms (TLBO, PSO and ABC). The nondimensional frequency responses and corresponding optimum lamination scheme are shown in Fig. 4 and Table 3 respectively. It is observed from the responses that the non-dimensional fundamental frequency values are following the increasing trend with the increase in the

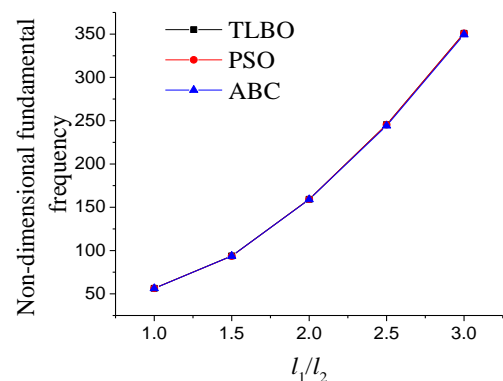


Fig. 4 Effect of plate aspect ratio on the non-dimensional fundamental frequency for simply-supported antisymmetric angle-ply laminated plates ($l_1/l_2 = 100$)

Table 2 Comparison study of fundamental frequency and orientations of eight-layer antisymmetric laminated composite plate with different boundary conditions ($l_1/l_3 = 1$)

Case	Edges BCs	Ω			Optimal Stacking		
		Narita (2006)	Bargh and Sadr (2012)	Present (PSO)	Narita (2006)	Bargh and Sadr (2012)	Present (PSO)
1	SSSS	56.32	56.37	56.39	(45°/-45°/45°/45°) ₂	(-45°/45°/46°/46°) ₂	(-45°/45°/44°/48°) ₂
2	SSSF	39.84	39.83	40.08	(0°/0°/0°/0°) ₂	(0°/0°/0°/0°) ₂	(0°/0°/0°/0°) ₂
3	SFSF	38.69	38.69	38.95	(0°/0°/0°/0°) ₂	(0°/0°/0°/0°) ₂	(0°/0°/0°/0°) ₂
4	SSCC	68.72	71.50	73.60	(0°/45°/-45°/-45°) ₂	(-42°/42°/-42°/42°) ₂	(44°/-45°/-45°/47°) ₂

Table 3 Effect of plate aspect ratio on the optimum lamination scheme for simply-supported angle-ply antisymmetric laminated plates ($l_1/l_3 = 100$)

Algorithm	l_1/l_2				
	1	1.5	2	2.5	3
TLBO	$(-45^\circ/45^\circ/44^\circ/48^\circ)_2$	$(64^\circ/-65^\circ/-69^\circ/84^\circ)_2$	$(-90^\circ/90^\circ/90^\circ/-90^\circ)_2$	$(-90^\circ/90^\circ/-90^\circ/-90^\circ)_2$	$(-90^\circ/90^\circ/90^\circ/-90^\circ)_2$
PSO	$(-45^\circ/45^\circ/45^\circ/45^\circ)_2$	$(66^\circ/-63^\circ/90^\circ/-61^\circ)_2$	$(90^\circ/-90^\circ/-90^\circ/-90^\circ)_2$	$(-90^\circ/90^\circ/90^\circ/90^\circ)_2$	$(90^\circ/90^\circ/-90^\circ/90^\circ)_2$
ABC	$(43^\circ/-41^\circ/-45^\circ/51^\circ)_2$	$(62^\circ/-65^\circ/-74^\circ/63^\circ)_2$	$(86^\circ/-87^\circ/-85^\circ/85^\circ)_2$	$(89^\circ/-87^\circ/89^\circ/-90^\circ)_2$	$(-89^\circ/-87^\circ/88^\circ/-88^\circ)_2$

aspect ratios irrespective of the different algorithms. This is because of the increase in structural stiffness (as the width is decreasing) with the increase in aspect ratio.

3.2.2 Effect of length-to-thickness ratio (l_1/l_3)

This example presents the dynamic responses for five length-to-thickness ratios ($l_1/l_3 = 10, 20, 50, 100$ and 150) of the square plate. The edges of the plate structure are considered to be simply-supported and the necessary responses obtained using all the three algorithms (TLBO, PSO and ABC) are presented in Fig. 5. In addition, the corresponding individual lamina orientation are tabulated in

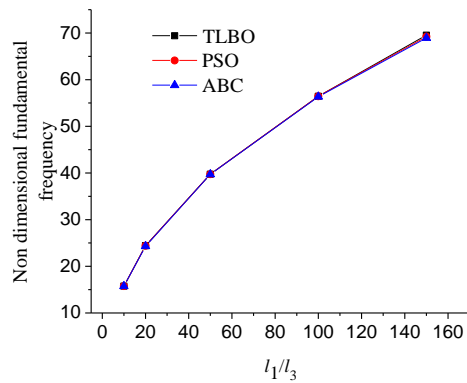


Fig. 5 Effect of plate length to thickness ratio on the non-dimensional fundamental frequency for simply-supported antisymmetric angle-ply laminated plates

Table 4. It is observed from the responses that the non-dimensional fundamental frequency values are following the increasing trend with increasing the length to thickness ratios. Additionally, it is worth to mention that the optimum lamination scheme remains unchanged with the increase in length to thickness ratios.

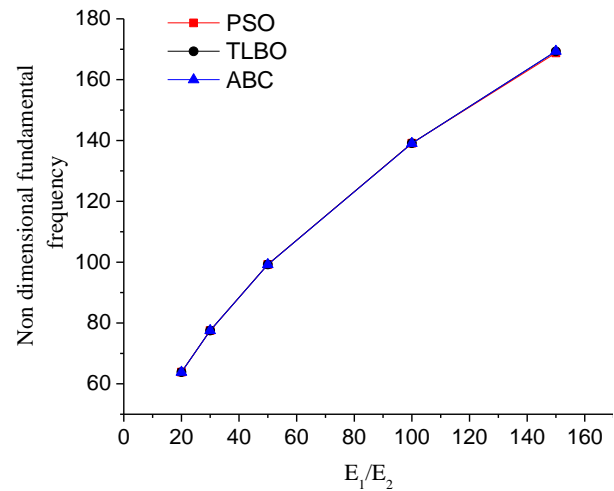


Fig. 6 Effect Young's modulus ratio on the non-dimensional fundamental frequency for simply-supported antisymmetric angle-ply laminated plates ($l_1/l_3 = 100$)

Table 4 Effect of plate length to thickness ratios on the optimum lamination scheme for simply-supported angle-ply antisymmetric laminated plates

Algorithm	l_1/l_3				
	10	20	50	100	150
TLBO	$(-45^\circ/45^\circ/45^\circ/-45^\circ)_2$	$(45^\circ/-45^\circ/-45^\circ/45^\circ)_2$	$(45^\circ/-45^\circ/45^\circ/-45^\circ)_2$	$(45^\circ/-45^\circ/45^\circ/44^\circ)_2$	$(45^\circ/-45^\circ/-45^\circ/45^\circ)_2$
PSO	$(-45^\circ/45^\circ/45^\circ/47^\circ)_2$	$(-45^\circ/44^\circ/45^\circ/-45^\circ)_2$	$(45^\circ/-45^\circ/45^\circ/-45^\circ)_2$	$(45^\circ/-45^\circ/45^\circ/-45^\circ)_2$	$(45^\circ/-45^\circ/45^\circ/-45^\circ)_2$
ABC	$(-45^\circ/43^\circ/-45^\circ/45^\circ)_2$	$(45^\circ/-45^\circ/-45^\circ/42^\circ)_2$	$(45^\circ/-45^\circ/-45^\circ/45^\circ)_2$	$(45^\circ/-44^\circ/45^\circ/-45^\circ)_2$	$(-44^\circ/-45^\circ/47^\circ/-46^\circ)_2$

Table 5 Effect of Young's modulus ratio ratios on the optimum lamination scheme for simply-supported angle-ply antisymmetric laminated plates ($l_1/l_3 = 100$)

Algorithm	l_1/l_3				
	20	30	50	100	150
TLBO	$(-45^\circ/45^\circ/45^\circ/-48^\circ)_2$	$(45^\circ/-45^\circ/46^\circ/-47^\circ)_2$	$(-45^\circ/44^\circ/46^\circ/-44^\circ)_2$	$(-45^\circ/45^\circ/44^\circ/-43^\circ)_2$	$(45^\circ/-45^\circ/-45^\circ/46^\circ)_2$
PSO	$(-45^\circ/45^\circ/45^\circ/-45^\circ)_2$	$(45^\circ/-45^\circ/-45^\circ/45^\circ)_2$	$(-45^\circ/-45^\circ/45^\circ/-45^\circ)_2$	$(-45^\circ/45^\circ/45^\circ/-45^\circ)_2$	$(45^\circ/-45^\circ/-45^\circ/45^\circ)_2$
ABC	$(-45^\circ/43^\circ/-45^\circ/45^\circ)_2$	$(45^\circ/-45^\circ/-45^\circ/42^\circ)_2$	$(45^\circ/-45^\circ/-45^\circ/45^\circ)_2$	$(45^\circ/-44^\circ/45^\circ/-45^\circ)_2$	$(-44^\circ/-45^\circ/47^\circ/-46^\circ)_2$

3.2.3 Effect of Young's modulus ratio (E_1/E_2)

In order to analyze the influence of the modular ratio nondimensional frequency values of the plate structure with simply-supported edges is evaluated in this illustration for different modular ratios ($E_1/E_2 = 20, 30, 50, 100$ and 150). The thickness ratio of the plate is considered as ($l_1/l_3 = 100$). The values obtained using all the three algorithms (TLBO, PSO and ABC) are shown in Fig. 6 and Table 5. The nondimensional frequencies are following the increasing trend as the modular ratio increases. The increase in frequency values is due to the increase in stiffness of the panel with the increase in modular ratios. Because the transverse modulus is considered to be constant in this example and the corresponding longitudinal modulus value increases when the modular ratio increase.

4. Conclusions

A hybrid model is developed by coupling the higher-order kinematic theory based FE model and three different optimization algorithms (TLBO, PSO and ABC) for the prediction of optimal stacking sequence and corresponding frequency values. The higher-order FE model is used to evaluate the eigenvalue responses, i.e., fundamental frequency and different optimization algorithm techniques for the prediction of the corresponding optimum lamination scheme. The final governing equation is obtained using the weak form finite element approach. The responses are computed numerically with the help of in-house computer code using the derived mathematical model in MATLAB-12 environment. Now, the necessary stability and the accuracy of the computed frequencies including the optimal sequences are completed as a priority and further utilized them to comprehensive parametric study. The detailed parameter dependent numerical nondimensional frequency values are following an increasing path for the increased value of the aspect ratios, the thickness ratios and the modular ratios. However, the frequency parameter not affected considerably while the values of the thickness ratios and the optimal fibre angle sequence increase. Finally, from the current optimisation study, it can be concluded that all three techniques have the capability of predict the responses without much deviations. But the convergence rate including the consistency of results obtained via all three techniques indicate the suitability over other two methods. This is because the responses obtained using all three methods follow the converge immediate after twenty steps for each methodologies but the predictions via TLBO is consistent and close convergence between two successive values.

References

- Aagaah, M.R., Mahinfalah, M. and Jazar, G.N. (2006), "Natural frequencies of laminated composite plates using third order shear deformation theory", *Compos. Struct.*, **72**(3), 273-279.
- Kumar, A., Kumar, V.R., Datta, S. and Mahapatra, S.S. (2017), "Parametric appraisal and optimization in machining of CFRP composites by using TLBO (teaching-learning based optimization algorithm)", *J. Intel. Manuf.*, **28**(8), 1769-1785.
- Apalak, M.K., Yildirim, M. and Ekici, R. (2008), "Layer optimisation for maximum fundamental frequency of laminated composite plates for different edge conditions", *Compos. Sci. Technol.*, **68**(2), 537-550.
- Apalak, M.K., Karaboga, D. and Akay, B. (2014), "The artificial bee colony algorithm in layer optimization for the maximum fundamental frequency of symmetrical laminated composite plates", *Eng. Optimiz.*, **46**(3), 420-437.
- Bargh, H.G. and Sadr, M.H. (2012), "Stacking sequence optimization of composite plates for maximum fundamental frequency using particle swarm optimization algorithm", *Meccanica*, **47**(3), 719-730.
- Chiu, L.N., Rolfe, B., Wu, X. and Yan, W. (2018), "Effect of stiffness anisotropy on topology optimisation of additively manufactured structures", *Eng. Struct.*
DOI: <https://doi.org/10.1016/j.engstruct.2018.05.083>
- Conti, P., Luparello, S. and Pasta, A. (1997), "Layer thickness optimisation in a laminated composite", *Compos. Part B: Eng.*, **28**(3), 309-317.
- Cook, R.D., Malkus, D.S., Plesha, M.E. and Witt, R.J. (2003), *Concepts and Applications of Finite Element Analysis*, John Wiley and Sons Pvt. Ltd, Singapore.
- Ding, Z., Lu, Z., Huang, M. and Liu, J. (2017), "Improved artificial bee colony algorithm for crack identification in beam using natural frequencies only", *Inverse Probl. Sci. Eng.*, **25**(2), 218-238.
- Eberhart, R.C. and Shi, Y. (2001), "Particle swarm optimization: Developments, Applications and Resources", *Proceedings of the 2001 Congress on Evolutionary Computation*, pp. 81-86.
- Fourn, H., Atmane, H.A., Bourada, M., Bousahla, A.A., Tounsi, A. and Mahmoud, S.R. (2018), "A novel four variable refined plate theory for wave propagation in functionally graded material plates", *Steel Compos. Struct., Int. J.*, **27**(1), 109-122.
- Grzywiński, M. (2015), "Optimization of double-layer braced barrel vaults", *Transactions of the VSB-Technical University of Ostrava, Civil Engineering Series*, **15**(2).
- Hajmohammad, M.H., Farrokhi, A. and Kolahchi, R. (2018), "Smart control and vibration of viscoelastic actuator-multiphase nanocomposite conical shells-sensor considering hygrothermal load based on layerwise theory", *Aerosp. Sci. Technol.*, **78**, 260-270.
- Ho-Huu, V., Do-Thi, T.D., Dang-Trung, H., Vo-Duy, T. and Nguyen-Thoi, T. (2016), "Optimization of laminated composite plates for maximizing buckling load using improved differential evolution and smoothed finite element method", *Compos. Struct.*, **146**, 132-147.
- Jones, R.M. (1999), *Mechanics of Composite Materials*, Taylor & Francis, PA, USA.
- Karaboga, D. and Basturk, B. (2008), "On the performance of artificial bee colony (ABC) algorithm", *Appl. Soft Comput.*, **8**(1), 687-697.
- Karami, B., Janghorban, M., Shahsavari, D. and Tounsi, A. (2018), "A size-dependent quasi-3D model for wave dispersion analysis of FG nanoplates", *Steel Compos. Struct., Int. J.*, **28**(1), 99-110.
- Kaveh, A. and Talatahari, S. (2009), "Particle swarm optimizer, ant colony strategy and harmony search scheme hybridized for optimization of truss structures", *Comput. Struct.*, **87**(5-6), 267-283.
- Kolahchi, R. (2017), "A comparative study on the bending, vibration and buckling of viscoelastic sandwich nano-plates based on different nonlocal theories using DC, HDQ and DQ methods", *Aerosp. Sci. Technol.*, **66**, 235-248.
- Kolahchi, R. and Bidgoli, A.M.M. (2016), "Size-dependent sinusoidal beam model for dynamic instability of single-walled carbon nanotubes", *Appl. Math. Mech. -Engl. Ed.*, **37**(2), 265-274.

- Kolahchi, R. and Cheraghbak, A. (2017), "Agglomeration effects on the dynamic buckling of viscoelastic microplates reinforced with SWCNTs using Bolotin method", *Nonlinear Dyn.*, **90**, 479-492.
- Kolahchi, R., Keshtegar, B. and Fakhar, M.H. (2017a), "Optimization of dynamic buckling for sandwich nanocomposite plates with sensor and actuator layer based on sinusoidal-viscopiezoelectricity theories using Grey Wolf algorithm", *J. Sandw. Struct. Mater.*
DOI: <https://doi.org/10.1177/1099636217731071>
- Kolahchi, R., Zarei, M.S., Hajmohammad, M.H. and Nouri, A. (2017b), "Wave propagation of embedded viscoelastic FG-CNT-reinforced sandwich plates integrated with sensor and actuator based on refined zigzag theory", *Int. J. Mech. Sci.*, **130**, 534-545.
- Mallick, P.K. (2007), *Fiber Reinforced Composites: Materials, Manufacturing and Design*, CRC press.
- Menasria, A., Bouhadra, A., Tounsi, A., Bousahla, A. A. and Mahmoud, S.R. (2017), "A new and simple HSDT for thermal stability analysis of FG sandwich plates", *Steel Compos. Struct.*, **25**(2), 157-175.
- Narita, Y. (2006), "Maximum frequency design of laminated plates with mixed boundary conditions", *Int. J. Solids Struct.*, **43**, 4342-4356.
- Omkar, S.N., Senthilnath, J., Khandelwal, R., Naik, G.N. and Gopalakrishnan, S. (2011), "Artificial Bee Colony (ABC) for multi-objective design optimization of composite structures", *Appl. Soft. Comput.*, **11**, 489-499.
- Patlle, B.K., Hirwani, C.K., Singh, R.P. and Panda, S.K. (2018), "Eigenfrequency and deflection analysis of layered structure using uncertain elastic properties – a fuzzy finite element approach", *Int. J. Approx. Reason.*, **98**, 163-176.
- Perera, R., Fang, S.E. and Ruiz, A. (2010), "Application of particle swarm optimization and genetic algorithms to multiobjective damage identification inverse problems with modelling errors", *Meccanica*, **45**(5), 723-734.
- Pati, R.P., Satpathy, M.P. and Satapathy, A. (2017), "Experimental investigation on Linz-Donawitz slag filled polypropylene composites using teaching-learning based optimization approach", *Polym. Compos.*
- Rao, R.V. and Patel, V.K. (2010), "Thermodynamic optimization of cross flow plate-fin heat exchanger using a particle swarm optimization algorithm", *Int. J. Therm. Sci.*, **49**, 1712-1721.
- Rao, R.V., Savsani, V.J. and Vakharia, D.P. (2011), "Teaching-learning-based optimization: A novel method for constrained mechanical design optimization problems", *CAD Comput. Aided Des.*, **43**, 303-315.
- Rao, R.V., Kalyankar, V.D. and Waghmare, G. (2014), "Parameters optimization of selected casting processes using teaching learning-based optimization algorithm", *Appl. Math. Model.*, **38**, 5592-5608.
- Sayare, R.S. and Kamble, A.G. (2015), "Parameter optimization of composite leaf spring using TLBO Algorithm", *Int. Eng. Res.*, 4358-4364.
- Stewart, R. (2009), "Carbon fibres composites poised for dramatic growth", *Reinf. Plast.*, **53**, 16-21.
- Tsavdaridis, K.D., Kingman, J.J. and Toropov, V.V. (2015), "Application of structural topology optimisation to perforated steel beams", *Comput. Struct.*, **143**, 108-123.
- Vo-Duy, T., Ho-Huu, V., Do-Thi, T.D., Dang-Trung, H. and Nguyen-Thoi, T. (2017), "A global numerical approach for lightweight design optimization of laminated composite plates subjected to frequency constraints", *Compos. Struct.*, **159**, 646-655.
- Vo-Duy, T., Truong-Thi, T., Ho-Huu, V. and Nguyen-Thoi, T. (2018), "Frequency optimization of laminated functionally graded carbon nanotube reinforced composite quadrilateral plates using smoothed FEM and evolution algorithm", *J. Compos. Mater.*, **52**(14), 1971-1986.
- Vosoughi, A.R., Forkhorji, H.D. and Roohbakhsh, H. (2016), "Maximum fundamental frequency of thick laminated composite plates by a hybrid optimization method", *Compos. Part B: Eng.*, **86**, 254-260.
- Zhang, L.G., Yang, K., Zhao, W.P. and Xiang, S. (2014), "Layer Thickness Optimization of Laminated Composite Plates to Maximize the First-Order Natural Frequency", *Appl. Mech. Mater.*, **709**, 139.

CC